Turkish Journal of Chemistry

http://journals.tubitak.gov.tr/chem/

Research Article

Turk J Chem
(2013) 37: 57 – 65

doi:10.3906/kim-1203-22

Electrochemical properties of 1,3-disubstituted methyl methoxy phenyl-5-phenylformazans and comparison with spectral properties

Habibe TEZCAN*, Güler EKMEKCİ, M. Levent AKSU
Department of Chemistry, Gazi Faculty of Education, Gazi University,
Teknikokullar, 06500 Ankara, Turkey

Received: 13.03.2012 • **Accepted:** 04.12.2012 • **Published Online:** 24.01.2013 • **Printed:** 25.02.2013

Abstract: In this study, electrochemical behaviors of formazans were investigated. The compounds contained CH_3 and OCH_3 groups at the *o*-, *m*-, and *p*-positions of the 1-phenyl ring and an OCH_3 group at the *p*-position of the 3-phenyl ring. Their electrochemical behaviors, such as the number of electrons transferred, diffusion coefficients, and heterogeneous rate constants, were studied by cyclic voltammetry, ultramicrodisk electrode, and chronoamperometry. Possible mechanisms were proposed based upon the data obtained. There was a correlation between the absorption and electrochemical properties. A linear correlation was obtained between λ_{max} and E_{red2} and Hammett substituent coefficients with E_{red2} and k_s values.

Key words: Formazans, substituent effect, cyclic voltammetry, ultramicrodisk electrode, chronoamperometry

1. Introduction

Formazans are colored compounds owing to the conjugated double bonds they contain. Since the first formazans were synthesized by Von Pechmann, numerous formazans have been synthesized and their structural properties and tautomeric and photochromic isomers have been investigated.[1–4] Their derivatives containing electron-donating and electron-withdrawing groups at the 1,3,5-phenyl rings were prepared and the effects of substituents on the absorption λ_{max} values and bond lengths, bond polarity, and crystal structures were determined.[5–8]

Formazans form tetrazolium salt when they are oxidized.[9] Tetrazolium salts are reduced back to formazans by the enzymes in the cell and stain the tissue. That is why the tetrazolium/formazan system is classified as a marker of vitality and used in the screening of anticancer drugs and in determination of activity on tumor cell and sperm viability.[10–13] This biological activity has caused increasing interest in the chemistry of formazans. Therefore, the investigation of their electrochemical features is very important.

A study carried out on the redox behavior of formazans revealed that tetrazolium salts are reduced to both mono- and diformazans by one-electron transfer. The first one-electron transfer results in the formation of a tetrazolium radical, and this radical undergoes the disproportionation reaction.[14] In polarographic study of formazans, there were 2 irreversible diffusion controlled processes, each with one-electron transfer.[15]

It was also reported that formazans are oxidized in a single 2-electron transfer, followed by a deprotonation reaction forming corresponding tetrazolium cation.[16] In a study of the reduction of tetrazolium salts into formazans with superoxide ions, which is claimed to cause aging and various diseases in the human body,

*Correspondence: habibe@gazi.edu.tr

there was one-electron transfer at –0.20 V (Ag/AgCl) and one-electron/one-proton transfer at –0.40 V.[17] In previous studies the synthesis and spectral and electrochemical behavior of some substituted formazans have been reported.[18–22]

In our previous study, 15 novel formazans were synthesized, their structures were identified, and the effect of substituents upon $\lambda_{\max}$ were also investigated.[19] In this study, the electrochemical behavior of the formazans containing CH_3 and OCH_3 groups at the $o-, m-$, and p-positions of the 1-phenyl ring and an OCH_3 group at the p-position of the 3-phenyl ring were investigated (Scheme 1), and their oxidation and reduction potentials (E_{ox}, E_{red}), the diffusion coefficients (D), number of electrons transferred (n), and standard heterogeneous rate constants (k_s) were determined. A mechanistic scheme is proposed based upon these data (Scheme 2).

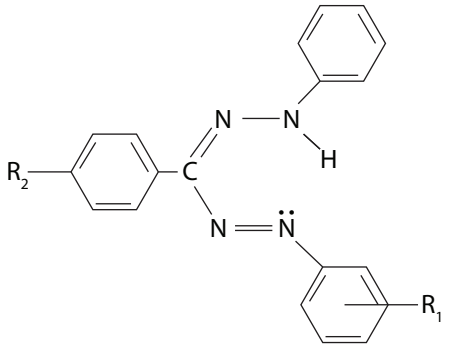

R1: R2: H (1)
R1: o- m- p-CH3; R2: p-OCH3 (2–4)
R1: o- m- p-OCH3; R2: p-OCH3 (5–7)

Scheme 1. The proposed structure of the formazans synthesized.

2. Experimental

2.1. Chemicals

1,3,5-Triphenylformazan and its derivatives 1-($o-, m-, p$-tolyl)-3-(p-methoxyphenyl)-5-phenylformazans (**2**–**4**) and 1-($o-, m-, p$-methoxyphenyl)-3-(p-methoxyphenyl)-5-phenylformazans (**5**–**7**) were prepared as described in the literature[19] and the compounds were purified by recrystallization until sharp melting points were obtained. The structures of the compounds were elucidated by using elemental analysis, GC-Mass, ^{1}H-NMR, ^{13}C-NMR, IR, and UV-Vis spectra, and spectral behaviors were investigated.[19]

All other chemicals were purchased from Merck and Sigma-Aldrich. The solvents used for synthesis were deionized water (Millipore, Milli-Q), CH_3OH (99.9%), CH_3COCH_3 (99.9%), and dioxane (99.9%), and the spectroscopic and electrochemical measurements were made by the use of absolute dry dimethyl sulfoxide (DMSO) (99.99%). The supporting electrolyte, tetrabutylammonium tetrafluoroborate (TBATFB), was purchased from Fluka (21796-4) and was used without purification and stored in a desiccator.

2.2. Measurements

Electrochemical studies were carried out with a computerized CHI Instrument 660 B system in a conventional 3-electrode cell. A platinum electrode (PE) (CHI102) and a 10 μm-platinum ultramicrodisk electrode (UME) (CHI107) were used as a working electrode. The real surface area of the Pt electrode was found to be 2.58 cm^2 by using ferrocene. Electrodes were thoroughly cleaned by electrochemical potential cycling and washing with

excess DMSO. A platinum wire was used as the auxiliary electrode and the reference electrode was a silver wire in contact with 0.1 M $AgNO_3$ prepared in dimethyl sulfoxide containing 0.1 M TBATFB. All solutions were deaerated for 10 min with pure argon. All the measurements were performed at 25 °C. Elemental analyses were carried out using a LECO-CHNS-932 elemental analyzer and mass spectra were recorded on an AGILENT 1100 MSD LC/MS spectrometer.

2.3. Method

The number of electrons transferred (n) and the diffusion coefficients (D) were determined from the Cottrell equation by the ultramicroelectrode CV technique of Baranski.[23] The heterogeneous rate constants k_s were calculated according to the Klingler–Kochi method.[24]

2.4. Information about formazans

Here, only the elemental analyses and molecular weights are given for the confirmation of the molecular structure of formazans. The UV-Vis data were used in order to compare them with the electrochemical results.[19]

1-(*o*−, *m*−, *p*-tolyl)-3-(*p*-methoxyphenyl)-5-phenylformazans (**2**–**4**): Elemental analysis for compound **2**, $C_{21}H_{20}N_4O$, Calc. (%): C, 73.25; H, 5.81; N, 16.28. Found: (%) C: 73.21: H, 5.76, N: 16.24. Calc M: 344. Found mass: m/z (eV): 345.1, 239.1, 225.0, 119.

1-(*o*−, *m*−, *p*-methoxyphenyl)-3-(*p*-methoxyphenyl)-5-phenylformazans (**5**–**7**): Elemental analysis of purple-colored compound **5**, $C_{21}H_{20}N_4O_2$, Calc. (%): C, 70.00; H, 5.55; N, 15.55. Found: (%) C: 70.06, H: 5.51, N: 15.62. Calc. M: 360, Found mass: m/z (eV) 361.1, 255.1, 225.1, 122.1.

3. Results and discussion

3.1. Characterization of the electrode reactions

The voltammograms were scanned over a potential range from –2000 to 0 mV in the positive direction in forward mode with a scan rate of 100 mV s^{-1}. The cyclic voltammograms of formazans substituted with CH_3 and OCH_3 at the *o*−, *m*−, and *p*-positions of the 1-phenyl ring and OCH_3 at the *p*-position of the 3-phenyl ring (**2**–**7**) are compared to the parent compound TPF (**1**) in Figures 1 and 2.

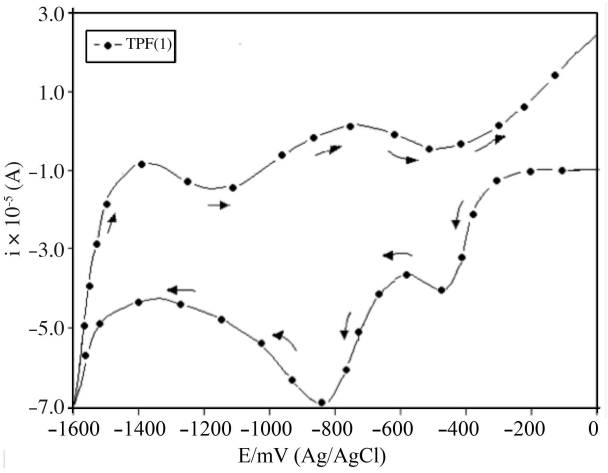

Figure 1. Cyclic voltammogram of a DMSO solution of 1.0×10^{-4} M TPF (**1**) in the presence of 0.1 M TBATFB at Pt electrode. Potential scan rate: 100 mV s^{-1}.

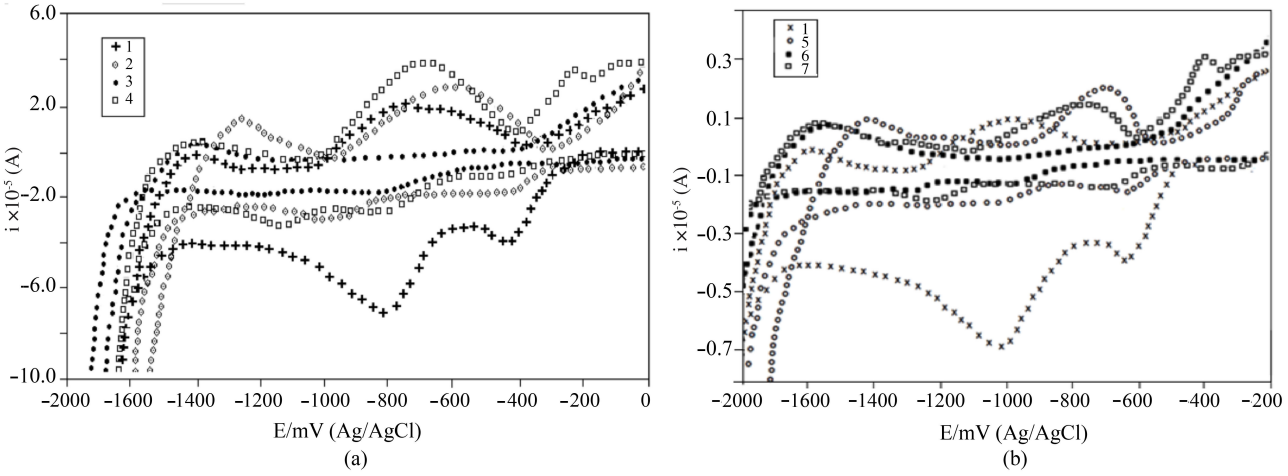

Figure 2. Cyclic voltammogram of DMSO solutions of 1.0 $\times$ 10^{-4} M compounds a) **1**–**4** and b) **1**, **5**–**7** in the presence of 0.1 M TBATFB at Pt electrode. Potential scan rate: 100 mV s^{-1}.

There were 2 major oxidation peaks in the cyclic voltammogram of TPF (**1**). In the first step, formazan releases 1 electron in the electrochemical reaction and 1 proton in the following chemical reaction (EC mechanism), corresponding to the formation of formazan radical ($TPF^{\bullet}$) at –1390.3 mV. In the second step, the radical gives another electron, resulting in a tetrazolium cation (TPT^{+}) at –740.7 mV. The reaction scheme can be depicted as follows.[14]

$TPF \rightarrow TPF^{\bullet} + e^{-}$ (electrode reaction)

$TPF^{\bullet} \rightarrow H^{+} + TPF^{\bullet}$ (chemical reaction)

$TPF^{\bullet} \rightarrow TPT^{+} + e^{-}$

It is clearly seen that the formation of radical from the compound is difficult, as indicated by the highly cathodic formation potential. However, the conversion of the radical into tetrazolium cation is much easier than radical formation. Therefore, the radical formation step is the rate-determining step. There are also 2 reduction peaks observed at –426.0 mV (E_{red1}) and –815.1 mV (E_{red2}) in reverse scan (Figure 1).

3.2. Oxidation of CH_3 substituted formazans

As seen from Figure 2a and Table 1, substitution of the 1-phenyl ring with the CH_3 group at the $o-$, $m-$, and p-positions (**2**–**4**) caused changes in both the peak potential and the peak currents as compared to the parent (**1**). The first oxidation peak potentials (E_{ox1}) were observed at –1264.1 mV, –1405.2 mV, and –1393.4 mV for **2**, **3**, and **4**, respectively. The second oxidation peak potentials (E_{ox2}) were observed at –614.8 mV and –703.7 mV for **2** and **4**, respectively. There was no E_{ox2} observed at the formazan of the m-position, as seen from Table 1 and Figure 2a. This may be due to the fact that both electrons are transferred in a single step.

There are reduction peaks in the opposite direction of oxidation reactions (Table 1; Figure 2a).The first reduction peak potentials (E_{red1}) were observed at –427.0 mV, –823.0 mV, and –856.6 mV for **2**, **3**, and **4**, respectively. It is obvious that there is cathodic shift in potential in the order of $o-<m-<p$-substitutions. This order is compatible with their absorption wavelengths (λ_{max}). They are in the order of $o- > m- > p- > CH_3$-substitute formazans. The second reduction peak potentials (E_{red2}) were observed at –952.3 mV and –1137.0 mV for **2** and **4**; however, there was no E_{red2} observed for the m-position. As the electron density decreases, the oxidation process becomes more difficult. The facts that there was extensive shift in E_{ox1} and that there were

no E_{ox2} or E_{red2} observed for the *m*-substituted compound can be attributed to the lower electron-releasing effect due to hyperconjugation.

Table 1. Electrochemical and kinetic data of formazans (**1**–**7**) in DMSO at 25 °C at platinum electrode, ionic strength: 0.1 M (TBATFB), scan rate: 100 mV s^{-1}. E_{ox}: oxidation; E_{red}: reduction, k_s (cm s^{-1}) values of column 11: ΔE_p: $E_{ox1} - E_{red2}$ (mV).

No	E_{ox1} (mV)	Ip_{ox1} (A) × 10^{-6}	E_{ox2} (mV)	Ip_{ox2} (A) × 10^{-6}	E_{red1} (mV)	Ip_{red1} (A) × 10^{-6}	E_{red2} (mV)	Ip_{red2} (A) × 10^{-6}	ΔE_p (mV)	k_s (cm s^{-1}) × 10^{-3}	λ_{max}
1	–1390.3	3.086	–740.7	1.789	–426.0	2.657	–815.1	6.098	565.2	7.722	482
2	–1264.1	15.510	–614.8	1.273	–427.0	18.180	–952.3	20.640	311.8	5.330	512
3	–1405.2	2.603	-	-	-	17.120	–823.0	-	582.2	7.035	504
4	–1393.4	4.245	–703.7	0.100	–856.6	26.330	–1137.0	32.150	255.8	40.500	501
5	–1215.1	9.288	–503.2	0.517	–464.5	15.160	–843.9	18.620	371.2	3.516	531
6	–1348.5	2.681	-	-	-	-	–1087.1	6.860	261.4	2.885	499
7	–1369.4	12.970	–561.3	2.600	–490.3	6.625	–1011.2	6.544	358.2	6.765	507

3.3. Oxidation of OCH_3 substituted formazans

The 2 oxidation peaks generally shifted to more anodic potentials in the substituted OCH_3 formazans (**5**–**7**) compared to TPF (**1**). The peak potentials (E_{ox1}) corresponding to the oxidation of formazan to formazan radical ($TPF^{\bullet}$) are –1215.1 mV, –1348.5 mV, and –1369.4 mV for **5**–**7**, respectively. The peak potentials (E_{ox2}) corresponding to the oxidation of formazan radical to tetrazolium cation (TPT^{+}) were –503.2 mV and –561.3 mV for **5** and **7**, respectively (Table 1; Figure 2b). There was not a distinctive peak for the *m*-position, which may be due to transfer of 2 electrons in a single step.

The peak potentials corresponding to the reduction of tetrazolium cation to formazan radical ($TPF^{\bullet}$) are –464.5 mV and –490.3 mV for **5** and **7,** respectively. The potentials of the second reduction peak (E_{red2}) were observed at –843.9 mV, –1087.1 mV, and –1011.2 mV for **5**–**7**, respectively.

The first oxidation peak potentials (E_{ox1}) shifted a little more in cathodic potentials in CH_3-substituted formazans (**2**–**4**) than in OCH_3-substituted formazans (**5**–**7**). The shifts are strikingly close to each other, which is not surprising since the Hammett constant contributions of CH_3 and OCH_3 are almost the same (Table 3).

This result is in agreement with spectroscopic results, as seen from Table 1. One can evaluate the rate of reaction by the use of cyclic voltammetric peak potentials. As seen from Table 1, the Ip_{ox1} value for *o*-CH_3 formazans (**2**) is 15.510 × 10^{-6} A, which is expected to give the highest rate of reaction. CH_3 exerts the highest electron donating effect at the *o*-position by the hyperconjugation, which is also supported by the k_s value given in Table 1.

In the case of OCH_3 substitution, the highest Ip_{ox1} value is observed for the *p*-position as 12.970 × 10^{-6} A. Therefore, the fastest reaction is expected to take place for the *p*-position. This is in complete accordance with the case that OCH_3 is electron-withdrawing by inductive effect and electron-donating by resonance effect. Inductive effect was extinguished from the *o*- to *p*- position. This case is supported by the Hammett substitution coefficients, σ. That is why the electron-donating effect is expected to be highest at the *p*-position, which causes the highest electron density and consequently eases the oxidation reaction. The k_s value given in Table 1 also verifies this fact.

3.4. Correlation between λ_{max} and E_{red2} vs. Ag/AgCl values

There was a correlation between absorption λ_{max} values of o-, m-, p-CH_3 and m-, p-OCH_3 substituted formazans (**2**–**4**, **6**, **7**) and their reduction peak potentials, E_{red2}. This was not the case for o-OCH_3 substituted formazan (**5**) (Figure 3). Consequently, both the absorption and the electrochemical features depend on the electron density of the molecular structure.

3.5. Ultramicrodisk electrode and chronoamperometric studies

The UME curves of formazans substituted with CH_3 and OCH_3 at the $o-$, $m-$, and p-positions of the 1-phenyl ring and OCH_3 at the p-position of the 3-phenyl ring (**2**–**7**) are compared to the parent compound TPF (**1**) in Figures 4a and 4b. These curves were taken in DMSO solutions of 1.0×10^{-4} M compounds **1**–**7** in the presence of 0.1 M TBATFB using a 10 μm-platinum ultramicroelectrode.

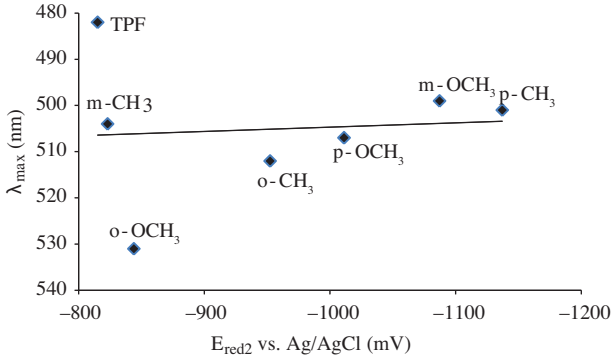

Figure 3. The correlation between the λ_{max_x} and E_{red2} vs. Ag/AgCl (mV) values.

The number of electrons transferred (n) and the diffusion coefficients (D) were determined by the ultramicroelectrode CV technique of Baranski.[23] The heterogeneous rate constants k_s were calculated according to the Klingler–Kochi method.[24] The k_s values under these circumstances depend on the scan rate, diffusion coefficient, and oxidation and reduction peak potential values. The n, D, and k_s values are tabulated in Tables 1 and 2.

Table 2. Some of the parameters calculated for formazans (**1**–**7**).

No	C* (mM)	I_{ss} (A) $\times 10^{-9}$	Cottrell slope (S $\times 10^{-5}$)	n	n net	D (cm^2 s^{-1}) $\times 10^{-6}$	λ_{max}
1	7.3	0.908	1.599	0.75	1	4.297	482
1	7.3	1.621	2.109	0.73	1	7.880	
2	6.4	0.671	1.487	1.24	1	2.717	512
2	6.4	0.604	1.712	0.86	1	2.446	
3	7.8	-	1.529	-	-	-	504
4	7.8	0.762	2.650	2.29	2	1.267	501
5	5.7	1.406	1.817	0.80	1	0.639	531
5	5.7	1.205	1.650	0.77	1	0.547	
6	6.5	-	1.999	-	-	-	507
7	6.8	1.492	3.325	2.12	2	2.842	499

The oxidation reactions of TPF and its CH_3 and OCH_3 derivatives appear to be irreversible, because ΔE_p (Ep^a – Ep^c) is larger than 59/n mV. As the scan rate increases, the anodic peak potentials also become

more anodic, the cathodic peak potentials become more negative, and ΔE_p increases. These results are consistent with irreversible behaviors.[25]

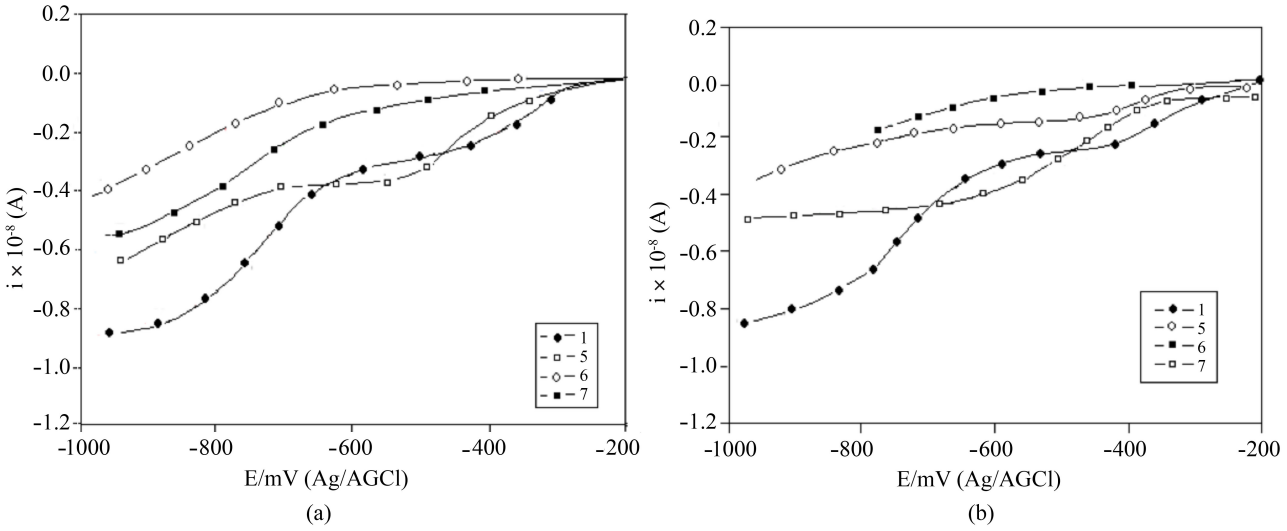

Figure 4. UME curves of DMSO solutions of 1.0 × 10^{-4} M compounds a) **1**, **2**–**4** and b) **1**, **5**–**7** in the presence of 0.1 M TBATFB at 10 μm-platinum ultramicroelectrode. Potential scan rate: 10 mV s^{-1}.

Table 3. The total σ_T $(\sigma_1 + \sigma_2)$ and related λ_{max} values.

Subs. posit.	No.	σ' values	σ_T (total)	$\lambda_{max\,1}$ (nm)	Chem. shift ($\Delta\lambda$)
	1	H: 0	0	482.0	
m-	**3**	*m*-CH_3: –0.06; *p*-OCH_3: –0.12	–0.18	504.0	–22
	6	*m*-OCH_3: 0.10; *p*-OCH_3: –0.12	–0.02	507.0	–25
p-	**4**	*p*-CH_3: –0.14; *p*-OCH_3: –0.12	–0.26	501.0	–19
	7	*p*-OCH_3: –0.12; *p*-OCH_3: –0.12	–0.24	499.0	–17

3.6. Studies on the reaction mechanism

If i_p values are plotted against $t^{-1/2}$, the resulting slope will be that from which n could be calculated. The numbers of electrons calculated are given in Table 2. As seen from the n value and the UME curves in Figure 4a and 4b, there was a 2-step-each one-electron transfer wave for the parent compound **1** and $o-CH_3$ and $o-OCH_3$ substituted formazans **2** and **5**. It is suggested that compounds first give 1 e^-, followed by 1 H^+ transfer, resulting in formazan radicals ($TPF^{\bullet}$). The resulting radical converts to tetrazolium cation (TTC^+) with 1 further e^- transfer. These results indicate that the mechanism is EC.[14] Mechanisms of the oxidation of these compounds are shown in Scheme 2a. These results are in agreement with literature findings.[17] There were one-step 2-electron transfer waves in the case of $m-$, $p-CH_3$ and $m-$, $p-OCH_3$ substituted formazans **3**, **4**, **6**, and **7**. The mechanisms of the oxidation of these compounds are shown in Scheme 2b. These results are in agreement with the literature findings.[16]

There was no certain trend between k_s and any other parameters, since they are also dependent upon the other factors. However, there was a correlation of E_{red2} and k_s with Hammett substitution coefficients σ_T (Table 3; Figures 5 and 6).

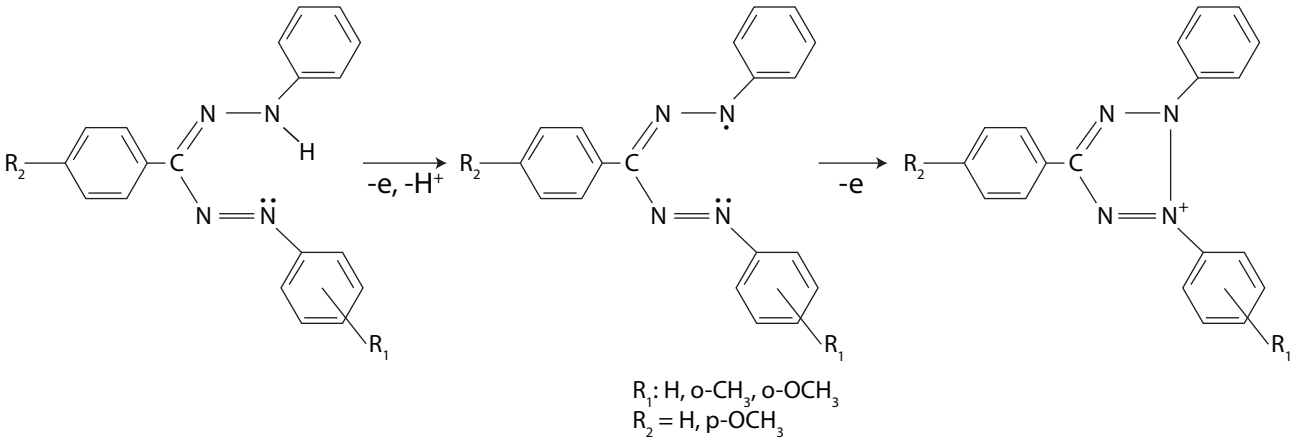

Scheme 2a. Possible oxidation mechanism of **1**, **2**, and **5**.

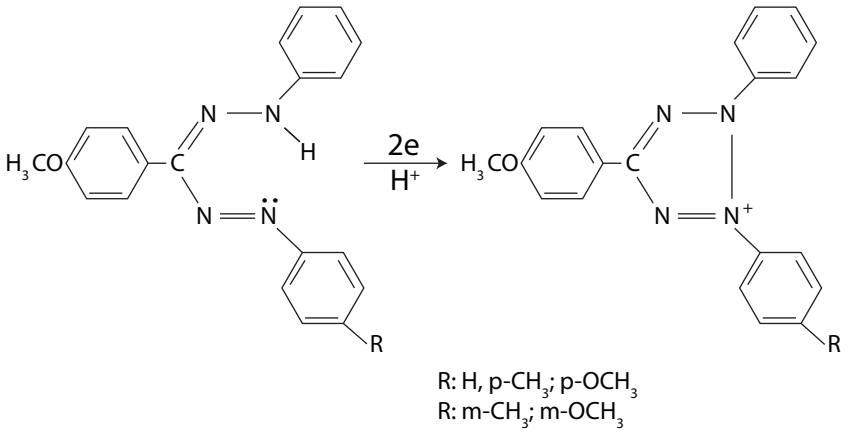

Scheme 2b. Possible oxidation mechanism of **3**, **4** and **6**, **7**.

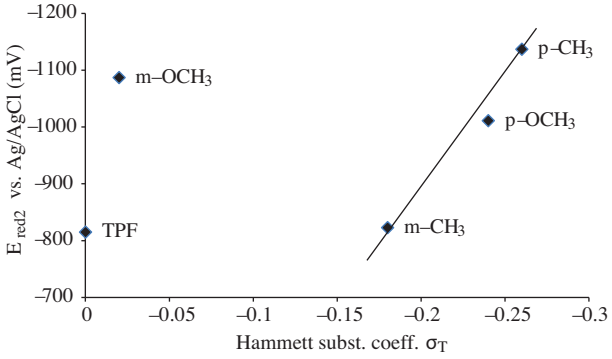

Figure 5. The correlation between E_{red2} vs. Ag/AgCl (mV) and Hammett substitution coefficients σ_T.

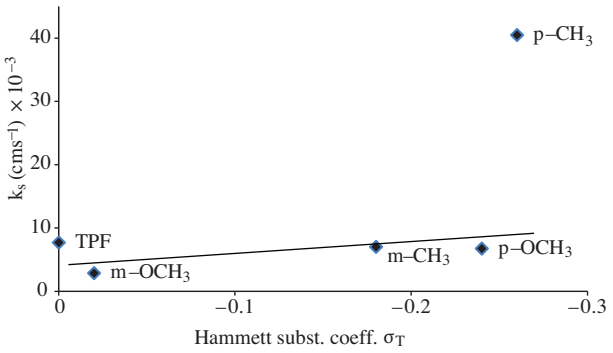

Figure 6. The relation between the k_s (cms^{-1}) $\times$ 10^{-3} and Hammett substituent coefficients σ_T.

4. Conclusions

Formazans were characterized with respect to their absorption and redox behavior. In spite of the fact that k_s is dependent on many other parameters, there was good correlation between the k_s values and Hammett substitution coefficients σ_T, and consequently absorption λ_{max}.

The reduction peak potentials E_{red2} also correlate well with Hammett substitution coefficients σ_T. This is an expected outcome since both the absorption and the electrochemical features are dependent on the electron density of systems.

It was observed that electron-releasing groups ease the oxidation reactions according to their positions on the ring. This was truly the case for o-CH_3-substituted and p-OCH_3-substituted compounds.

The oxidation of formazans to tetrazolium cations is irreversible as indicated by the CV data. The mechanistic scheme of the compounds is dependent upon the type and the position of the substituent on the rings.

Acknowledgments

The authors are grateful to the Gazi University Research Fund for providing financial support for this project (No. 04/ 2004-13).

References

1. Pechmann, H. Von. *Ber. Detsch. Chem. Ges.* **1894**, *27*, 1679.
2. Hunter, L.; Roberts, C. B. *J. Chem. Soc.* **1941**, *9*, 820–823.
3. Lewis, J. W.; Sandorfy, C. *Can. J. Chem.* **1983**, *61*, 809–816.
4. Katritzky, A. R.; Belyakov, S. A.; Cheng, D.; Durst, H. D. *Synthesis* **1995**, *5*, 577–581.
5. Yüksel U. Postdoctoral Thesis, Ege University, 1981, in Turkish.
6. Tezcan, H.; Can, S.; Tezcan, R. *Dyes and Pigments* **2002**, *52*, 121–127.
7. Tezcan, H.; Ozkan, N. *Dyes and Pigments* **2003**, *56*, 159–166.
8. Erkoc, S.; Tezcan, H.; Calisir, E. D.; Erkoc, F. *Int. J. Pure Applied Chem.* **2006**, *1*, 37–44.
9. Schiele, V. C. *Ber.* **1964**, *30*, 308–318.
10. Mattson, A. M.; Jensen, C. O.; Dutcher, R. A. *Science* **1947**, *5*, 294–295.
11. Plumb, J. A.; Milray, R.; Kaye, S. B. *Cancer Res.* **1989**, *49*, 4435–4440.
12. Wan, H.; Williams, R.; Doherty, P.; Williams, D. F. *J Mater. Sci. Mater. M.* **1994**, *5*, 154–159.
13. Aziz, D. M. *Anim. Reprod. Sci.* **2006**, *92*, 1–8.
14. Umemoto, K. *Bull. Chem. Soc. Jpn.* **1989**, *62,* 3783–3789.
15. Viseu, M. I.; Simoes Goncalves, M. L. S.; Costa, S. M. B.; Ferreira, M. I. C. *J. Electroanal. Chem.* **1990,** *282*, 201–214.
16. Abou Elenien, G. M. *J. Electroanal. Chem.* **1994**, *375*, 301–305.
17. Oritani, T.; Fukuhara, N.; Okajima, T.; Kitamura, F.; Ohsaka, T. *Inorg. Chim. Acta* **2004**, *357*, 436–442.
18. Göke, G.; Durmus, Z.; Tezcan, H.; Yılmaz, H.; Kılı, E. *Anal. Sci.* **2005**, *21*, 685–688.
19. Tezcan, H.; Uzluk, E. *Dyes and Pigments* **2007**, *75*, 633–640.
20. Tezcan, H.; Uzluk, E.; Aksu, M. L. *Spectrochim. Acta A* **2008**, *69*, 971–979.
21. Tezcan, H.; Uzluk, E.; Aksu, M. L. *J. Electroanal. Chem.* **2008**, *619–620*, 105–116.
22. Tezcan, H.; Uzluk, E.; Aksu, M. L. *Electrochim. Acta* **2008**, *53*, 5597–5607.
23. Baranski, A. S.; Fawcett, W. R.; Gilbert, C. M. *Anal. Chem.* **1985**, *57*, 166–170.
24. Klingler, R. J.; Kochi, J. K. *J. Phys. Chem.* **1981**, *85*, 1731–1741.
25. Bard, A. J.; Faulkner, L. R. *Electrochemical Methods: Fundamentals and Applications*, 2001, John Wiley and Sons, New York.